ANTIOXIDANTS & REDOX SIGNALING
Volume 18, Number 14, 2013

DOI: 10.1089/ars.2012.4799

Therapeutics

FORUM ORIGINAL RESEARCH COMMUNICATION

Superoxide Dismutase Mimetic, MnTE-2-PyP, Attenuates Chronic Hypoxia-Induced Pulmonary Hypertension, Pulmonary Vascular Remodeling, and Activation of the NALP3 Inflammasome

Leah R. Villegas,[1,2] Dylan Kluck,[1] Carlie Field,[1] Rebecca E. Oberley-Deegan,[3] Crystal Woods,[1] Michael E. Yeager,[1,2] Karim C. El Kasmi,[1,2] Rashmin C. Savani,[4] Russell P. Bowler,[3] and Eva Nozik-Grayck[1,2]

Abstract

Aims: Pulmonary hypertension (PH) is characterized by an oxidant/antioxidant imbalance that promotes abnormal vascular responses. Reactive oxygen species, such as superoxide ($O_2^{\bullet -}$), contribute to the pathogenesis of PH and vascular responses, including vascular remodeling and inflammation. This study sought to investigate the protective role of a pharmacological catalytic antioxidant, a superoxide dismutase (SOD) mimetic (MnTE-2-PyP), in hypoxia-induced PH, vascular remodeling, and NALP3 (NACHT, LRR, and PYD domain-containing protein 3)–mediated inflammation. ***Results:*** Mice (C57/BL6) were exposed to hypobaric hypoxic conditions, while subcutaneous injections of MnTE-2-PyP (5 mg/kg) or phosphate-buffered saline (PBS) were given 3× weekly for up to 35 days. SOD mimetic-treated groups demonstrated protection against increased right ventricular systolic pressure, indirect measurements of pulmonary artery pressure, and RV hypertrophy. Vascular remodeling was assessed by Ki67 staining to detect vascular cell proliferation, α-smooth muscle actin staining to analyze small vessel muscularization, and hyaluronan (HA) measurements to assess extracellular matrix modulation. Activation of the NALP3 inflammasome pathway was measured by NALP3 expression, caspase-1 activation, and interleukin 1-beta (IL-1β) and IL-18 production. Hypoxic exposure increased PH, vascular remodeling, and NALP3 inflammasome activation in PBS-treated mice, while mice treated with MnTE-2-PyP showed an attenuation in each of these endpoints. ***Innovation:*** This study is the first to demonstrate activation of the NALP3 inflammasome with cleavage of caspase-1 and release of active IL-1 β and IL-18 in chronic hypoxic PH, as well as its attenuation by the SOD mimetic, MnTE-2-PyP. ***Conclusion:*** The ability of the SOD mimetic to scavenge extracellular $O_2^{\bullet -}$ supports our previous observations in EC-SOD-overexpressing mice that implicate extracellular oxidant/antioxidant imbalance in hypoxic PH and implicates its role in hypoxia-induced inflammation. *Antioxid. Redox Signal.* 18, 1753–1764.

Introduction

Excess production of reactive oxygen species (ROS) such as superoxide ($O_2^{\bullet -}$) contributes to the pathogenesis in human pulmonary hypertension (PH) and animal models of PH (8, 14, 29, 44). PH can complicate hypoxic lung diseases (WHO Group III PH), increasing morbidity and mortality. Loss of vascular antioxidant protection against $O_2^{\bullet -}$ contributes to vascular remodeling and development of PH in several animal models including chronic hypoxia-induced PH, and represents an important target for antioxidant strategies. A pharmacological catalytic antioxidant and superoxide dismutase (SOD) mimetic, Mn(III)tetrakis(N-ethylpyridinium-2-yl)porphyrin (MnTE-2-PyP), protects the lung in several experimental models of lung injury and inflammation, but its impact in models of PH has not been evaluated (5, 7, 34).

[1]Department of Pediatrics and [2]Cardiovascular Pulmonary Research, University of Colorado, Aurora, Colorado.
[3]Department of Medicine, National Jewish Health, Denver, Colorado.
[4]Division of Pulmonary & Vascular Biology, Department of Pediatrics, University of Texas Southwestern Medical Center, Dallas, Texas.

Innovation

Antioxidants are an important defense system in fibrotic and inflammatory diseases, and the use of new antioxidant strategies may be useful as therapeutic tools or in the research setting to identify new pathways important in the pathogenesis of disease. The antioxidant superoxide dismutase mimetic, Mn(III)tetrakis(N-ethylpyridinium-2-yl)porphyrin (MnTE-2-PyP), exhibits important properties, as it has been shown to target extracellular ROS, which we propose are central to pulmonary vascular remodeling. In this study, we demonstrated a protective effect of MnTE-2-PyP on the regulation of the extracellular matrix component HA, which is not only a key matrix component, but also can itself promote inflammation. We then focused on a newly recognized pathway, the NACHT, LRR, and PYD domain-containing protein 3 inflammasome, which is responsible for caspase-1 activation and interleukin 1-beta (IL-1β) and IL-18. This inflammatory system is central to a number of chronic inflammatory diseases, but has not been well explored in human pulmonary arterial hypertension or animal models of pulmonary hypertension. Overall, our study is novel in its focus on extracellular events and the identification of new pathways amenable to therapeutic interventions.

MnTE-2-PyP belongs to a class of catalytic antioxidants and functions as an SOD mimetic. SOD antioxidant enzymes scavenge $O_2^{\bullet -}$ by catalyzing the dismutation of two $O_2^{\bullet -}$ radicals into hydrogen peroxide and oxygen (12, 26). As a metalloporphyrin, MnTE-2-PyP is a metal ion chelator that mimics the dismutation of $O_2^{\bullet -}$ by alternate reduction and oxidation reactions between MN(III) and MN(II) within its extensive conjugated ring system (36). Pharmacokinetic studies of metalloporphyrins show that this compound is distributed at moderate levels to the lungs (AUC = 26.5 μ*h/ml) and heart (AUC = 14.8 μg*h/ml) in mice that were given a single intraperitoneal dose of 10 mg/kg (42). Maximum concentration is reached within 45 min and a slow elimination phase allowed a half-life of 60 to 135 h. Using these characterizations, we have developed a dosing regimen to study the effects of the SOD mimetic in chronically hypoxic mice. MnTE-2-PyP is an attractive agent to test, as SOD mimetics have been shown to effectively block oxidative stress in acute lung injury and attenuate bleomycin-induced pulmonary fibrosis, a model also used to study secondary PH (7, 34). While SOD mimetics can scavenge both intracellular and extracellular $O_2^{\bullet -}$ (43, 49), we specifically investigated the potential contributions of extracellular protection by analyzing two extracellular targets of $O_2^{\bullet -}$, the extracellular matrix (ECM) component hyaluronan (HA) and an inflammatory pathway in macrophages, the NALP3 inflammasome.

The ECM is susceptible to oxidative damage and changes in the ECM contribute to the development of PH by regulating structural properties of the vessel and promoting inflammation (17, 20, 27, 37, 40). Extracellular antioxidant enzymes such as extracellular superoxide dismutase (EC-SOD) protect against oxidative damage to the ECM (13, 28). To test whether MnTE-2-PyP can protect against events in the extracellular vascular compartment, we chose to test one important matrix component and a potentially related inflammatory pathway. One relevant target of extracellular $O_2^{\bullet -}$ is HA, a key component of the ECM (13, 49, 50). Fragmented HA is detected in the lung fluid and serum of patients with idiopathic pulmonary arterial hypertension (PAH) (1, 35), suggesting that oxidative damage to the vascular ECM may be a contributing factor in hypoxic PAH.

Chronic inflammation is also now well recognized to contribute to PH, and is both regulated by ROS and contributes to ROS production. Relevant to this study, pro-inflammatory cytokines interleukin 1-beta (IL-1β) and IL-18 have been implicated in lung diseases, including PAH (4, 19, 25, 41). It has recently been determined that the NALP3 inflammasome is central to the activation of IL-1β and IL-18 (22, 23, 45). This protein platform that includes the NOD-like receptor, NALP3 (NACHT, LRR, and PYD domain-containing protein 3), is a component of the innate immune system that regulates the activation of caspase-1 and subsequently IL-1β and IL-18 (48). The NALP3 inflammasome has not been previously characterized in models of PH and, based on its role in processing of IL-1β and IL-18, serves as a rationale to study targets of extracellular $O_2^{\bullet -}$ potentially amenable to antioxidant treatment with AEOL 10113.

Based on the utility of MnTE-2-PyP to target extracellular $O_2^{\bullet -}$, we hypothesized that treatment with MnTE-2-PyP would protect against the development of chronic hypoxic pulmonary hypertension (CHPH), vascular remodeling, and inflammation.

Results

SOD mimetic attenuates CHPH

We first established that the SOD mimetic, MnTE-2-PyP, protected against CHPH in mice. Phosphate-buffered saline (PBS)-treated mice exposed to hypobaric hypoxia for 35 days developed increases in right ventricular systolic pressure (RVSP) (Fig. 1A). Treatment with the SOD mimetic attenuated the hypoxia-induced elevation in pulmonary arterial pressures. The SOD mimetic also blunted the hypoxia-induced increase in RV hypertrophy (Fig. 1B).

SOD mimetic attenuates pulmonary vascular remodeling

An established feature of CHPH is pulmonary vascular remodeling. We therefore evaluated cell proliferation in the vessel wall, muscularization of small vessels, and HA content, a key ECM component in the adventitia susceptible to oxidative fragmentation.

Pulmonary artery cell proliferation and muscularization

Our previous studies have shown a transient increase in pulmonary artery cell proliferation at early hypoxic time points (3 days) followed at later time points by small vessel muscularization (21 or 35 days) (32). Ki67 nuclear staining and alpha smooth muscle actin (α-SMA) staining were used as markers to quantify the number of proliferating cells and the number of muscularized vessels at the relevant time points, 3 and 21 days, respectively (Fig. 2A, B). In response to a 3-day hypoxic exposure, mice had increased numbers of proliferating cells within the medial and intimal layers of similar-sized pulmonary arteries (50–200 μm) compared to normoxic controls (image taken at 20× magnification). Hypoxia-exposed mice

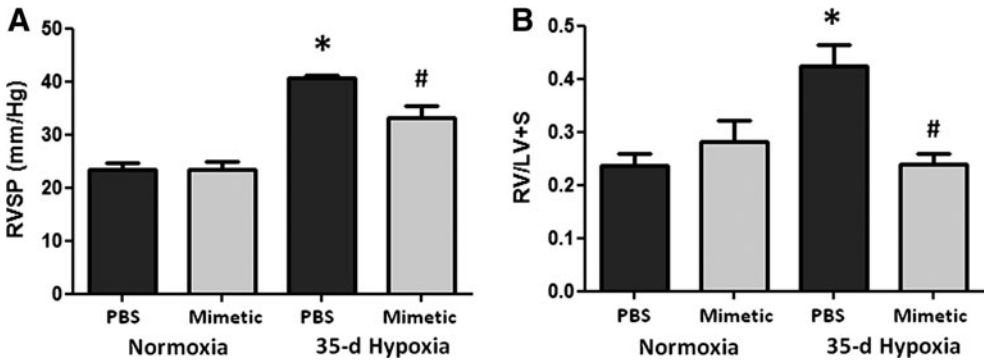

FIG. 1. SOD mimetic attenuates chronic hypoxia-induced pulmonary hypertension. (A) Chronic hypoxic pulmonary hypertension was assessed by direct right ventricle (RV) puncture and measurement of RV systolic pressure (RVSP) in 35-day hypoxic mice treated with SOD mimetic and compared to hypoxia-exposed mice treated with PBS and normoxic controls. **(B)** RV hypertrophy was assessed by right ventricle/left ventricle + septum weights. $^{*}p < 0.05$ compared to normoxic groups; $^{\#}p < 0.05$ compared to PBS treated groups. $n = 4$ to 6 mice per group.

treated with SOD mimetic had less proliferating cells in the pulmonary arteries (Fig. 2C). The development of muscularized small ($< 50\,\mu$m) pulmonary vessels was also seen in response to 21 days of chronic hypoxia in PBS-treated mice. Treatment with the SOD mimetic attenuated the hypoxia-induced development of muscularized vessels (Fig. 2D).

Modulation of HA content

Oxidative stress in the lung can cause deposition and fragmentation of several components of the ECM, contributing to matrix remodeling (13, 28, 32, 49). Since HA content and activity is dependent upon its oxidative fragmentation, its

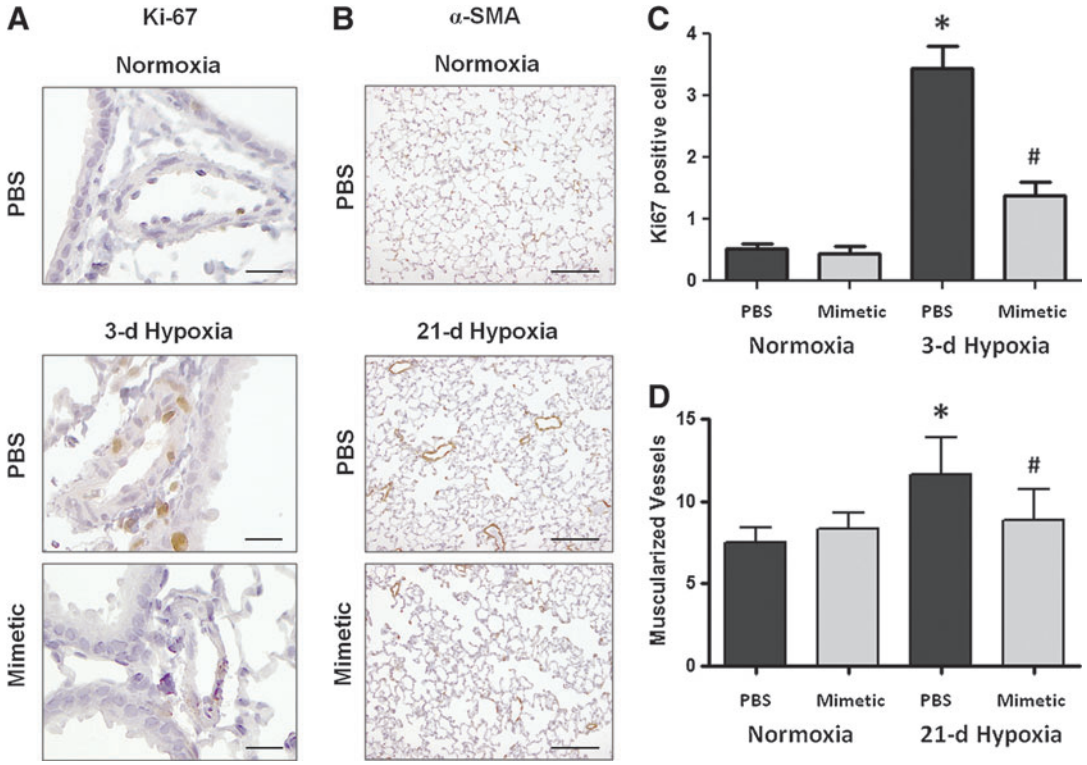

FIG. 2. Superoxide dismutase (SOD) mimetic attenuates hypoxia-induced early vascular cell proliferation and late vascular muscularization. Cell proliferation and muscularization of small pulmonary vessels evaluated by immunohistochemistry staining using **(A)** Ki67 and **(B)** α-smooth muscle actin (α-SMA) antibodies, respectively, in lung sections of hypoxic mice treated with SOD mimetic and compared to hypoxia exposed mice treated with PBS and normoxic controls. Ki67 images were taken at 20× magnification (scale bars represent 50 μm) and α-SMA images were taken at 10× magnification (scale bars represent 100 μm). **(C)** Cell proliferation at 3 days was quantified by counting the number of Ki67-positive cells within the medial and intimal layer of pulmonary arteries ($< 100\,\mu$m). **(D)** Vessel muscularization at 35 days was quantified by counting the number of fully muscularized small vessels ($< 50\,\mu$m), which have >75% of the vessel circumference stained with α-SMA. $^{*}p < 0.05$ compared to normoxic groups; $^{\#}p < 0.05$ compared to phosphate-buffered saline (PBS)-treated groups. $n = 4$ to 6 mice per group.

synthesis and degradation, and its main target receptor, CD44, we measured HA content and transcript expression of the HA receptor, CD44 (Fig. 3A), HA synthases (HAS1 and HAS2), and hyaluronidases (Hyal1 and Hyal2) (Fig. 3B). We observed time-dependent changes in the PBS-treated hypoxic mice in each of these measurements, while none of these parameters changed at any time point in hypoxic mice treated with the SOD mimetic. In PBS-treated groups, hypoxia caused an initial decrease in HA content followed by increased content after longer hypoxic exposure. Hypoxia also caused an initial increase in CD44 and hyaluronidase expression followed by decreased expression after longer hypoxic exposures. In SOD mimetic-treated groups, there were no significant changes in HA content or gene expression upon hypoxic exposure, except for decreased HAS1 transcript. Visualization of HA content in lung sections showed that HA was localized within the pulmonary arteries of normoxic and hypoxic mice (Fig. 3C).

SOD mimetic attenuates hypoxia-induced NALP3 inflammasome activation

We tested the impact of the SOD mimetic on a recently recognized inflammatory pathway, the NALP3 inflammasome-dependent activation of IL-1β and IL-18.

NALP3 expression

In whole lung homogenates, there was increased *NALP3* transcript expression as early as after a 3-day hypoxic exposure, with a further increase at 21 days of hypoxic exposure, followed by a subsequent decline in expression by 35 days of hypoxic exposure (Fig. 4A). In hypoxia-exposed mice that were treated with SOD mimetic, there was up to two-fold attenuation of *NALP3* transcript expression. Accordingly, immunoprecipitation analysis of NALP3 protein showed a significant increase after 21 days of hypoxia (Fig. 4B). Comparison of the NALP3 protein at the 21-day hypoxic time point showed less NALP3 expression in SOD mimetic-treated mice (Fig. 4C). Protein expression at the 35-day hypoxic time point was also analyzed, but no differences between the groups were seen (data not shown). However, despite differences in NALP3 expression only noted up to 21 days, differences in bound caspase-1 protein and IL-1β and IL-18 were seen at the 35-day hypoxic time point.

Caspase-1, IL-1β, and IL-18

To assess the activation of caspase-1 in this pathway, we quantified pro- and cleaved caspase-1 bound to the immunoprecipitated NALP3. Caspase-1 protein (either pro- or cleaved) was minimally detected in NALP3 immunoprecipitates from normoxic mice. Following 21 and 35 days of chronic hypoxia, pro-caspase-1 and cleaved caspase-1 expression in mouse lung was increased significantly (Fig. 5A). There was an attenuation of both forms of caspase-1 expression in hypoxic mice treated with SOD mimetic compared to PBS controls (Fig. 5B). Western blots of tissue lysates without immunoprecipitation showed no changes upon hypoxic exposure, further supporting the concept that NALP3 activation involves the binding of caspase-1 (Fig. 5A). Hypoxia increased *IL-1β* and *IL-18* transcript expression, whereas SOD mimetic treatments attenuated *IL-1β* expression but not *IL-18* expression (Fig. 6A, B). Caspase-1, IL-1β, and IL-18 protein expression after a 21-day hypoxic exposure did not significantly

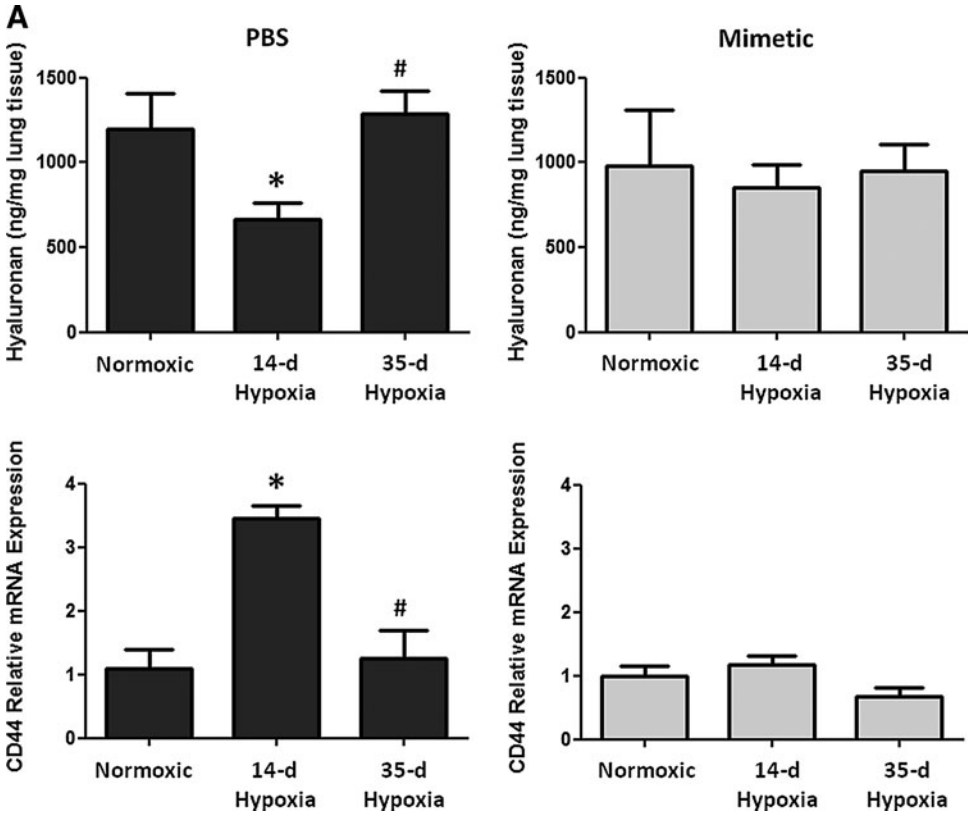

FIG. 3. Hyaluronan content in pulmonary vasculature is modulated by hypoxia. (A) Hyaluronan content and hyaluronan receptor (CD44) expression was measured in whole lungs of normoxic, 14-day hypoxic, and 35-day hypoxic mice treated with SOD mimetic or PBS. **(B)** Measurement of hyaluronidase (Hyal1 and Hyal2) and hyaluronan synthase (HAS1 and HAS2) expression. **(C)** Visualization of hyaluronan (HA) content in the vascular adventitia in the lungs of normoxic and hypoxic mice at 40× magnification (scale bars represent 100um). $^{*}p<0.05$ compared to normoxic groups; $^{\#}p<0.05$ compared to 14-day HX groups; $+p<0.06$ compared to normoxic groups. $n=3$ to 6 mice per group.

increase (data not shown). However, after a 35-day chronic hypoxic exposure, there was increased IL-1β and a trend toward increased IL-18 protein. Importantly, treatment with the SOD mimetic in 35-day hypoxia-exposed mice significantly decreased both IL-1β and IL-18 production compared to the 35-day hypoxic PBS-treated group.

Discussion

This study demonstrated that chronic hypoxic PH was attenuated in mice treated with MnTE-2-PyP. This is of importance because MnTE-2-PyP has been shown to target both intracellular and extracellular superoxide (43, 49) in contrast

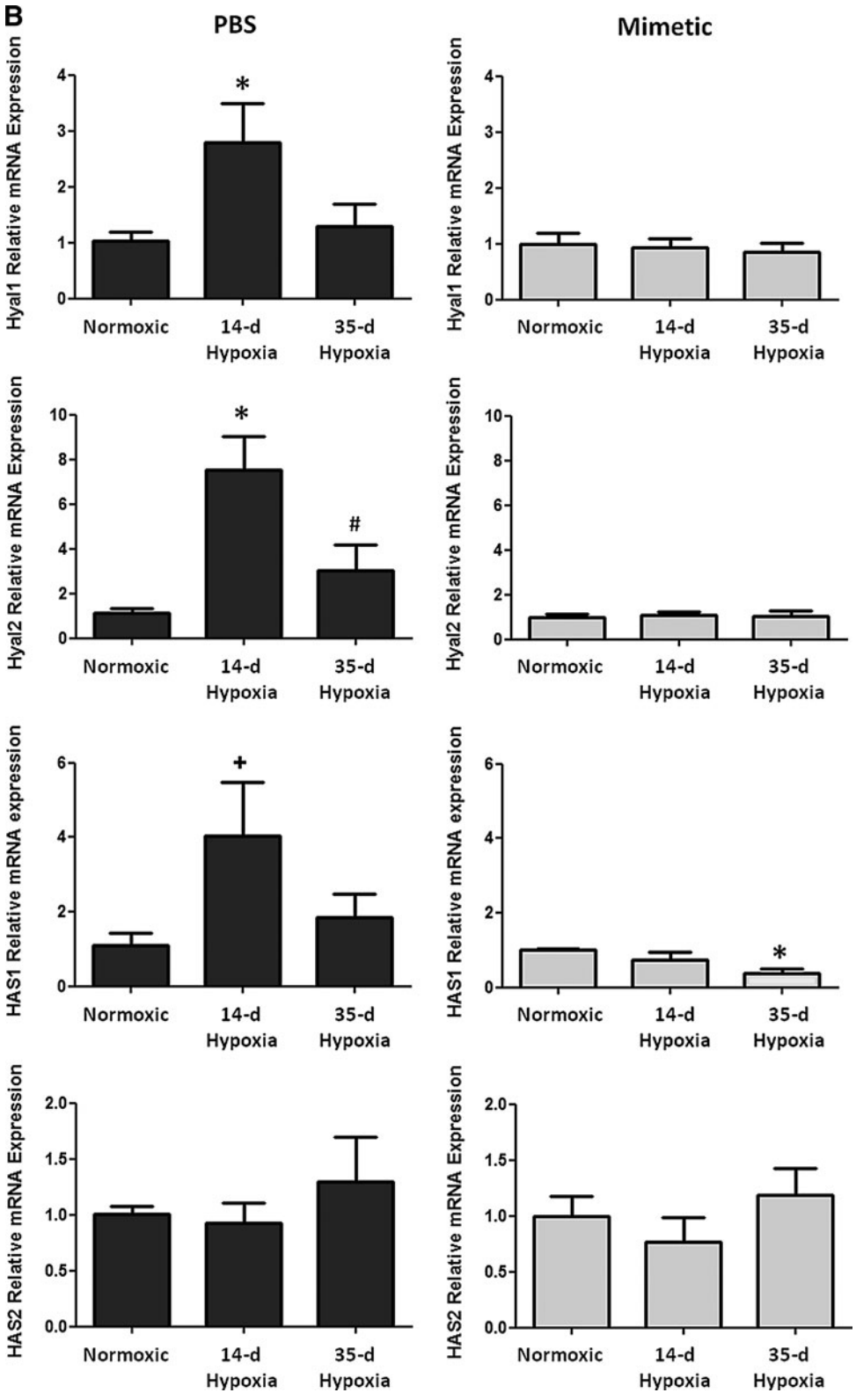

FIG. 3. (Continued).

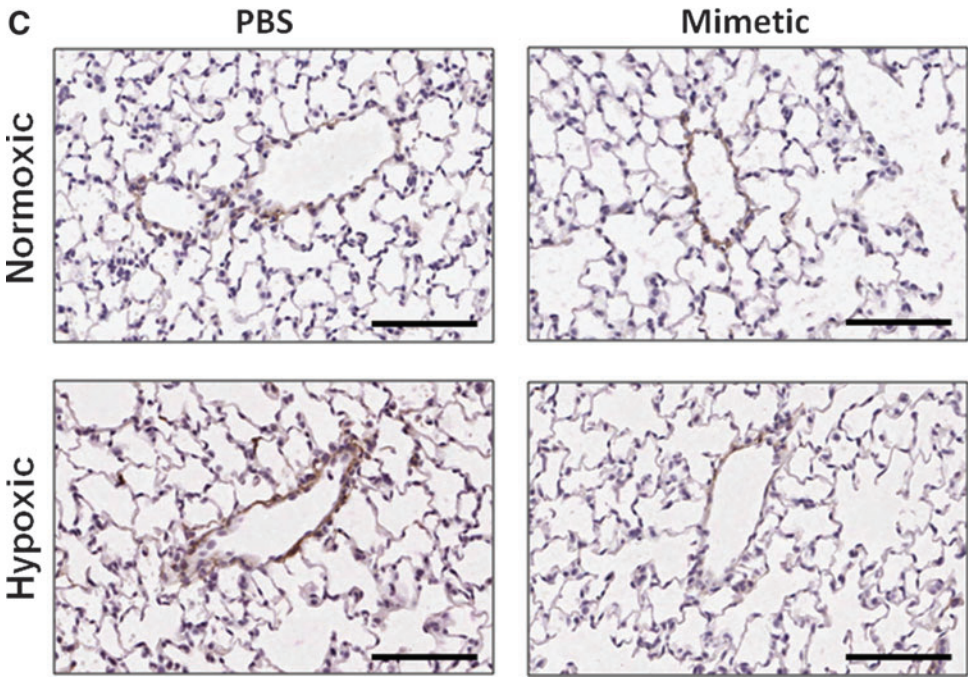

FIG. 3. (Continued).

with other tested antioxidant strategies, including tempol and allopurinol (9, 21, 38, 39). We are particularly interested in its role as an extracellular superoxide scavenger because of compounding evidence that support the critical role of extracellular oxidative stress and EC-SOD in oxidative pulmonary injury. EC-SOD is the major antioxidant enzyme in blood vessels, and recent studies have shown that chronic hypoxia causes decreased EC-SOD expression and activity in the lung (16, 32). Loss of EC-SOD contributes to the pathogenesis of PH, which provided the rationale to test antioxidant strategies that restore extracellular SOD activity in the vasculature (47). In addition, increased oxidative stress in mouse lungs is protected either by overexpression of lung EC-SOD (32) or adenoviral administration (6, 24) in chronic hypoxic or monocrotaline induced PH models. SOD mimetics are protective in other models of lung injury that are also associated with reduced EC-SOD expression (3, 11, 15). Our studies demonstrated that the extracellular properties of MnTE-2-PyP contribute to its protective effects in hypoxia-induced oxidative stress in pulmonary arteries, which lead us to further investigate two novel extracellular targets, HA and the NALP3 inflammasome.

Since this mimetic is a positive charged antioxidant similar to EC-SOD that scavenges superoxide and reverses diseases characterized by insufficient EC-SOD, it has been most commonly described as an EC-SOD mimetic. Although the activity has been shown to predominantly be SOD activity, the mimetic also has a low amount of catalase activity, scavenging hydrogen peroxide generated after the dismutase of superoxide. The catalase activity can be attributed to the ability of the Mn moiety to undergo higher oxidation states, such as Mn IV or Mn V, and thus converting hydrogen peroxide into water and oxygen. The advantages of this mimetic are its higher efficacy to dismutate superoxide (log kcat = 7.76 as compared to log kcat = 8.84–9.3 of SOD enzymes), its high efficacy to reduce peroxynitrite, (log kred = 7.53), and also scavenge carbonate radical. The ability to eliminate superoxide, peroxynitrite, and carbonate radical exceeds that of other compounds presently in preclinical and clinical studies such as Mn salen derivatives, Mn cyclic polyamines, nitrones, nitroxides, MitoQ, and similar compounds (36). One of our hypotheses focused on protection of extracellular remodeling that is linked to inflammation, *via* HA- and CD44-mediated activation of the NALP3 inflammasome.

MnTE-2-PyP protects against both early and late processes indicative of hypoxia-induced vascular remodeling, showing by its attenuation of early vessel wall cell proliferation and late small vessel muscularization. These findings support the premise that the extracellular compartment plays a critical role in vascular remodeling. One key finding demonstrated that HA, an important ECM component in the lung vasculature, was modulated in response to hypoxic exposure, and was suppressed by treatment with MnTE-2-PyP. In normal and healthy conditions, HA exists as intact, large-molecular-weight glycosaminoglycan polymers in the vascular adventitia. Upon lung injury, fragmented HA can be found in other compartments such as the bronchoalveolar lavage fluid and serum of patients with idiopathic pulmonary arterial hypertension (1, 35). In bleomycin lung injury, a model of PH, mice overexpressing EC-SOD had attenuated release of pulmonary HA into the bronchoalveolar fluid (50). HA content is regulated within a more intricate system, involving HA synthases and hyaluronidases. Published studies show that isolated IPAH pulmonary artery smooth muscle cells (PASMC) contained more HA in the culture supernatants compared to control donors and that HA content is associated with increased hyaluronan synthase (Has1) and decreased hyaluronidase (Hyal1) gene expression in the PASMC (1, 35). Fragmented HA can have a number of actions through different macrophage receptors that ultimately increase NALP3 inflammasome activation and interleukin release. Fragmented HA binds to the CD44 receptor to activate NALP3 inflammasome; the Rhamm receptor on macrophages to promote macrophage recruitment; and TLR4 to increase

NF-kB and IL gene expression (30). Our data suggest that hypoxia caused initial degradation of intact HA, while HA synthesis may have begun in response to longer hypoxic exposure. In addition, our data show that the HA receptor, CD44, which binds fragmented HA and can activate the NALP3 inflammasome, is also initially upregulated. HA content or CD44 expression in the SOD mimetic-treated groups did not change upon hypoxic exposure, suggesting that antioxidant treatment may stabilize HA modulation. MnTE-2-PyP may impact other extracellular signals or intracellular ROS that regulate NALP3 inflammasome activation independent of HA and we expect that these effects could be modulated by other antioxidants as well. Further studies are needed to elucidate the role of HA production, degradation, and source of HA fragments in chronic hypoxic PH. Regardless, the overall modulation of HA content in the lung is an important contributing factor because it is known to be involved in the activation of inflammatory pathways such as the NALP3-mediated production of IL-1β and IL-18.

MnTE-2-PyP attenuates IL-1β and IL-18 production, important lung cytokines that perpetuate inflammation, oxidative stress, and the development of PH. Studies have shown that IL-1β plays a role within a complex inflammatory environment in the pulmonary vascular remodeling process that involves inflammatory cell recruitment, proliferation of smooth muscle and endothelial cells, and mitochondrial and ion channel dysregulation (4, 18). Although other models show that early inflammation markers (46) precede hypoxia-induced PH, interestingly, our studies show that IL-1β and IL-18 are activated at a later time point. Changes in *IL-1β* transcript expression and protective effects of MnTE-2-PyP may be attributed to direct activation by extracellular ROS (31), or by a HA-TLR4 receptor signaling pathway, *via* the HA receptor CD44 and assembly of the NALP3 inflammasome (48). The NALP3 inflammasome is a component of the innate immune system and is responsible for caspase-1 dependent activation and secretion of IL-1β and IL-18 (2, 10, 31, 33, 45). Our data show that hypoxia induces caspase-1-mediated activation of the NALP3 inflammasome and subsequent production of IL-1β and IL-18, and that this response was attenuated by MnTE-2-PyP. Critical mechanisms involved in the pathogenesis of pulmonary vascular remodeling include modulation of the ECM and inflammation, two processes that are linked to oxidative stress in the lung. Because small molecular weight HA can act as endogenous signals to also activate the NALP3 inflammasome, our studies provide a rationale for further investigation into the contribution of extracellular HA as an activator of the NALP3 inflammasome in CHPH models. It may also inhibit other inflammatory pathways. For example, it has been shown that the SOD mimetic alters NF-kB by oxidizing one of the subunits and inhibiting its ability to bind to DNA. It has also been shown that the SOD mimetic inhibits AP-1 and HiF-1alpha, thus inhibit-

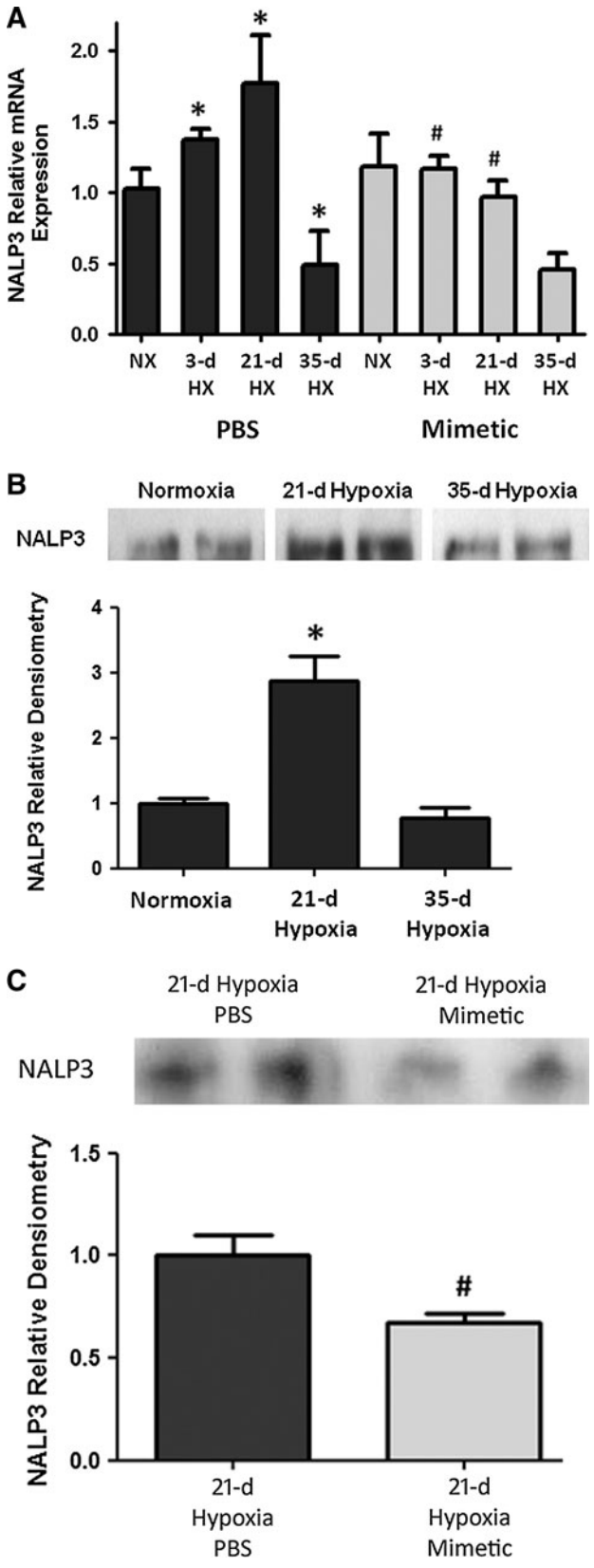

FIG. 4. SOD mimetic attenuates hypoxia-induced NALP3 expression. (A) Semi-quantitative PCR measurement of NACHT, LRR, and PYD domain-containing protein 3 (*NALP3*) transcript expression in hypoxic and normoxic mice treated with SOD mimetic or PBS. **(B)** Immunoprecipitation and Western blot, and densitometric analysis of NALP3 protein expression of normoxic and hypoxic mice. **(C)** NALP3 protein expression of 21-day hypoxic mice treated with SOD mimetic or PBS control is shown. $*p < 0.05$ compared to normoxic groups; $\#p < 0.05$ compared to PBS-treated groups. $n = 4$ mice per group. Blots shown are representative lanes of each group from the same blot.

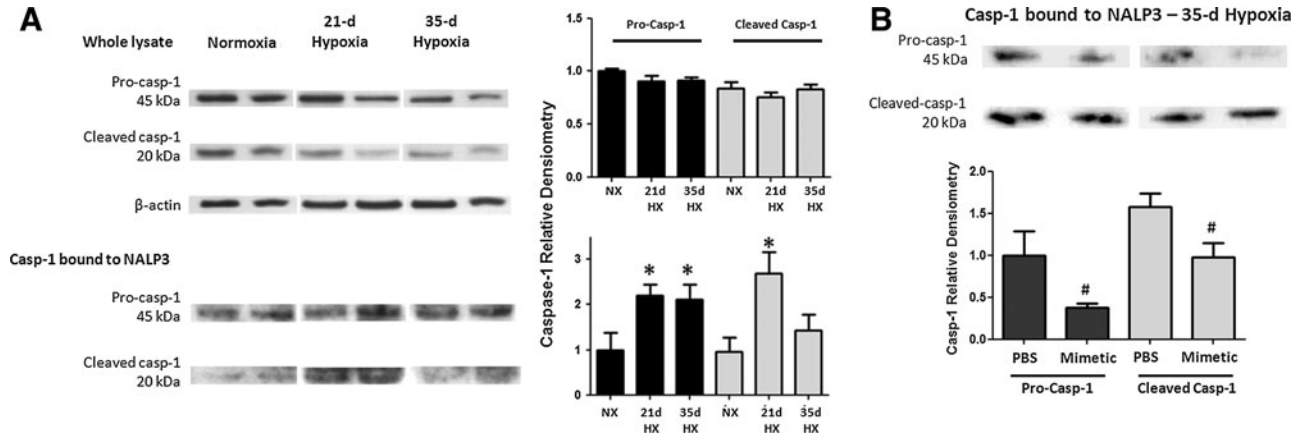

FIG. 5. SOD mimetic attenuates downstream Caspase-1 activation. (A) Hypoxia-induced pro- and cleaved caspase-1 expression in lung lysates. Protein bound to the inflammasome protein complex was quantified by immunoprecipitation of NALP3 and probing with caspase-1 antibody, producing 45-kDa pro-caspase-1 and 20 kDa cleaved caspase-1 bands. **(B)** Immunoprecipitates of 35-day hypoxic mice treated with SOD mimetic or PBS control. $^{*}p < 0.05$ compared to normoxic group; $^{\#}p < 0.05$ compared to PBS-treated groups. $n = 4$ mice per group. Blots shown are representative lanes of each group from the same blot.

ing inflammatory pathways directly. This study has provided a foundation to study pathways by which antioxidant replacement can impact inflammation, in this case, NALP3-mediated inflammation in CHPH, and further studies are needed to fully characterize this pathway.

In summary, our studies demonstrate that the SOD mimetic, MnTE-2-PyP, has a protective role in hypoxia-induced inflammation, pulmonary vascular remodeling, and development of PH. We have identified potential novel targets of oxidative stress in chronic hypoxia in the extracellular compartment that are modulated by MnTE-2-PyP. Future studies will evaluate the mechanisms inducing HA regulation and inflammasome activation, and provide a foundation to consider the therapeutic use of catalytic antioxidants for hypoxia-associated lung diseases.

Materials and Methods

Hypoxic mouse model and SOD mimetic treatment

Studies were performed on 4-week-old, C57/BL6 male mice (Jackson Lab, Bar Harbor, ME) maintained in normobaric normoxia or hypobaric hypoxia for up to 35 days. The

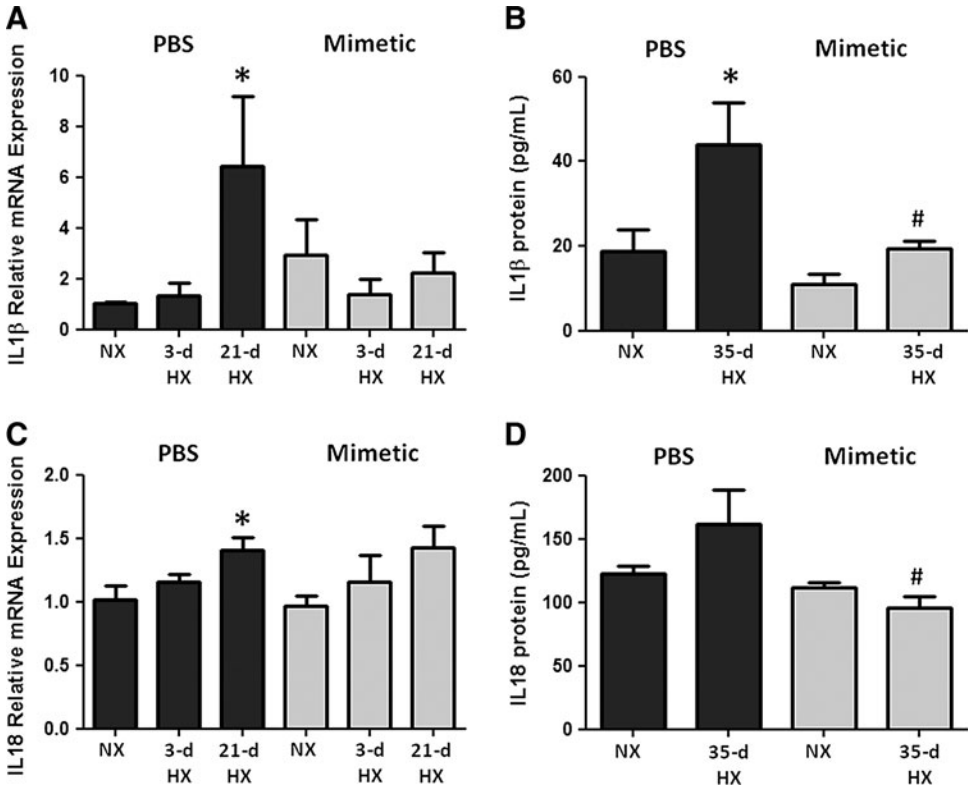

FIG. 6. SOD mimetic attenuates upregulation of interleukin 1-beta (IL-1 β) and IL-18 expression. *IL-1β* **(A)** transcript levels in whole lung homogenates of normoxic, 3-day hypoxic, and 21-day hypoxic mice treated with SOD mimetic or PBS measured by semi-quantitative PCR and **(B)** protein levels in treated normoxic and 35-day hypoxic mice measured by ELISA. *IL-18* **(C)** transcript and **(D)** protein. $^{*}p < 0.05$ compared to normoxic groups; $^{\#}p < 0.05$ compared to PBS-treated groups. $n = 4$.

hypoxia exposures were performed in hypobaric chambers at a simulated altitude of 18,000 ft above sea level (395 torr), conditions equivalent to 10% atmospheric oxygen. Normobaric conditions were at ~1500 ft above sea level (Denver, CO). Subcutaneous injections of phosphate buffered saline (PBS) or 5 mg/kg of SOD mimetic (MnTE-2-Pyp) dissolved in PBS were given three times weekly beginning on day 1 of hypoxic exposure or under normoxic conditions. Hemodynamic measurements and lung tissue were taken at the 3-, 21-, and 35-day time points according to the protocols as described below. Animal studies were approved by the Institutional Animal Care and Use Committee.

Assessment of PH

Mice were anesthetized by inhaled isofluorane (2%–4%) mixed with room air (21% oxygen, 79% nitrogen). RVSP was measured by direct RV puncture in a closed chest. A 25-gauge needle attached to a pressure transducer was introduced into the RV and live pressure tracings were measured using the Cardiomax III Cardiac Output program (Columbus Instruments). Pressures were monitored for at least 30 s, and averaged every 10 s to account for beat-to-beat variability. The blood was then drained from the lungs and heart by flushing 5 ml cold PBS into the right atrium and through the left atrium. The hearts were resected, and the right and left ventricle (including the septum) were separated under a dissecting microscope and then weighed. Right ventricular hypertrophy was quantified by comparing the ratio of the right ventricular/left ventricular + septum weights (RV/LV + S).

Measurement of vascular cell proliferation and muscularization

Lungs were flushed through the pulmonary artery with PBS, and then tissue was inflation fixed, embedded, and sectioned for immunohistochemistry according to previous methods (32). Briefly, the left lung was inflation-fixed at 20 cm H_2O pressure in 4% paraformaldehyde for 30 min and then dissected from the chest cavity and placed in 4% paraformaldehyde at 4°C for 2 days. Lungs were then transferred to 70% ethanol, paraffin-embedded, and sectioned. Lung sections were immunostained with monoclonal Ki67 antibody (1:200 Lab Vision NeoMarkers) or mouse monoclonal α-smooth muscle actin antibody (1:100, Clone 1A4). The block, secondary antibody, and avidin–biotin complex (ABC) reagent were provided in the Mouse-on-Mouse kit (Vector Laboratories) for the mouse monoclonal antibodies. The slides were developed with ImmPact DAB diluent (Vector Laboratories) and counterstained with hematoxylin. Tissue sections were examined by light microscopy and photographed. The number of proliferating Ki67-positive cells within the vessel wall was measured by counting Ki67-positive cells within the intimal and medial layer of muscularized pulmonary arteries between 50 and 150 μm (20× magnification). Ten vessels were counted for each mouse lung. The number of small vessels (<50 μm) with positive α-SMA staining was counted in 10 fields of view (10× magnification) to evaluate muscularized small pulmonary vessels. The analysis of Ki67 and α-SMA staining was evaluated by an investigator blinded to treatment groups.

Detection of HA content in mouse lung

HA content was measured from flushed and flash-frozen right lung tissue, using a competitive binding assay. This assay measures the competition of HA present in the sample verses HA coated on a 96-well plate for binding to a biotinylated HA-binding protein (bHABP Seikagaku). About 60 μL of sample or Healon standard (Pharmacia) was loaded onto nonfat dry milk-blocked Covalink-NH 96-Microwell plates (Nunc, Fisher Corp.) after overnight protease digestion. After addition of 60 μL bHABP to each well and incubation at 37°C for 1 h, 100 μL of the sample-bHABP incubation solution was transferred to a HA-coated Covalink plate and incubated for 1 h at 37°C to allow to competitive binding (0.2 mg/ml HA, ICN, Inc.). HA-binding was detected by an ABC reagent (Vectastain) and o-phenylenediamine (Sigma). The change in absorbance at 450 nm after a 15-min incubation was measured.

To visualize HA content around pulmonary vessels, inflation fixed, and embedded lungs were sectioned and stained. Lung sections were deparaffinized with citrisolve and rehydrated in graded ethanol. Negative controls were treated with hyaluronidase (Sigma) at a concentration of 1.5 μg/ml in sodium acetate buffer for 2 h at 60°C. Slides were blocked with Avidin/Biotin blocking kit (Vector Laboratories) and 0.1% BSA in PBS. Biotinylated HA-binding protein (Calbiochem) was then incubated on the slides overnight at 4°C at a concentration of 25 μg/ml in PBS. Slides were then washed with PBS, treated with 0.3% hydrogen peroxide, and then developed with Elite ABC reagent, Impact DAB, and hematoxylin QS (Vector Laboratories).

NALP3, IL-1β, *and* IL-18 *transcript expression*

RNA was isolated from frozen lungs to quantify *NALP3, IL-1β,* and *IL-18* transcript expression by semi-quantitative RT-PCR. RNA was extracted using RNeasy RNA isolation kit (Qiagen). Semi-quantitative PCR was performed using cDNA generated from 1 μg RNA. Enzymes and reagents used were Maxima First Strand cDNA Synthesis kit and Maxima SYBR Green/Fluorescein qPCR Master Mix (Fermentas). The threshold cycle for each sample in triplicate was measured using the Bio-Rad MyiQ™ Real-Time PCR Detection System. The PCR conditions used were 1 cycle at 95°C for 3 min and 60 cycles at 95°C for 30 s, 56°C for 30 s, and 72°C for 30 s. All transcripts were normalized to the endogenous control transcript, hypoxanthine phosphoribosyltransferase 1 (HPRT). Values are reported as transcript levels relative to the normoxic PBS group. The following primer sets were used: m*NALP3* forward 5′-GGTTG GTGAGCTGCTGTCTCACATC-3′, m*NALP3* reverse 5′-CTGT GTCTCCAAGGGCATTGCTTC-3′; m*IL1β* forward 5′-CTCCA CCTCAATGGACAGAATATCAACC-3′, m*IL1β* reverse 5′-GG TGGGTGTGCCGTCTTTCATTAC-3′; m*IL18* forward 5′-GGA CTGGCTGTGACCCTCTCTGTG-3′, m*IL18* reverse 5′-CAAAC TCCATCTTGTTGTGTCCTGGAAC-3′; m*HPRT* forward 5′-TG CTCGAGATGTCATGAAGGAG-3′, m*HPRT* reverse 5′-TTTAA TGTAATCCAGCAGGTCAGC-3′.

NALP3, Caspase-1, IL-1β, and IL-18 protein expression

Protein was isolated from frozen lungs to quantify NALP3, Caspase-1, IL-1β, and IL-18 expression by immunoprecipitation, Western blot, and ELISA. Protein was extracted by homogenizing lung samples in RIPA buffer with protease inhibitors (Sigma) for immunoprecipitation and Western blot or in T-PER buffer with protease inhibitors

(Pierce Biotechnology) for ELISA assays. For Western blot analysis, 30 μg total protein was loaded onto the gel. For immunoprecipitation, 200 μg total protein was immunoprecipitated using 2 μg NLRP3/NALP3 mouse IgG2b (Enzo Life Sciences) and goat anti-mouse IgG Magnabind beads (Pierce Biotechnology). Samples were applied to a magnet to separate protein bound to beads, and then washed eight times. After the last wash, protein was eluted using NuPage LDS sample buffer and reducing agent (Invitrogen). Samples were loaded on a 4%–12% Bis-Tris Gel and separated by electrophoresis (NuPAGE MES SDS Running Buffer; Invitrogen) and then transferred to a polyvinylidene difluoride membrane using the semi-dry method (NuPAGE Transfer Buffer; Invitrogen). The membranes were blocked for 1 h at room temperature with 5% milk in TBST buffer (0.05% Tween 20) and then probed with primary antibody, NLRP3/NALP3 mouse IgG2b (1:500 dilution; Enzo Life Sciences), or Anti-Caspase-1/ICE rabbit polyclonal (1:1000 dilution; Invitrogen), overnight at 4°C. Membranes were then incubated in HRP-conjugated secondary antibody (1:10,000 dilution), goat anti-mouse IgG, or goat anti-rabbit IgG (Millipore), for 1 h at room temperature. Blots were developed using SuperSignal West Femto Chemiluminescent Substrate (Thermo Scientific) and exposure to film. Band intensities were quantified by densiometry. For immunoprecipitated samples, band intensities were normalized to total protein of each sample (200 μg). For nonimmunoprecipitated samples, band intensities were normalized to β-actin. Densitometric analysis was reported as values relative to the normoxic or PBS control groups.

For ELISA assays, 100 μg total protein was loaded onto IL-1β- or IL-18-coated 96-well plates (eBioscience) and processed according to manufacturer's protocol. The absorbance was read at 450 nm. The concentration of each sample was extrapolated from mouse IL-1β or IL-18 recombinant protein standard curve.

Statistical analysis

For animal studies, we used $n = 4$ to 6 for each group. Assays were performed at least in triplicates to generate the mean and the standard error of the mean. The data comparing multiple groups were first analyzed by ANOVA, followed by Bonferonni post-test and Student's two-group t-test to evaluate differences between means of each group. $p < 0.05$ defines statistically significant differences.

Acknowledgments

We would like to thank James D. Crapo for helpful discussions and for supplying the SOD mimetic, MnTE-2-PyP. We would also like to thank Hagir B. Suliman and Kurt R. Stenmark for constructive feedback, and Jie Liao for excellent technical assistance. This work was funded by NIH grant R01-HL086680 to E.N.G., as well as R01-HL093535 and a grant from The Children's Medical Center Foundation to R.C.S. L.R.V. was supported by institutional training grant T32-HL007171.

Author Disclosure Statement

No competing financial interests exist.

References

1. Aytekin M, Comhair SAA, de la Motte C, Bandyopadhyay SK, Farver CF, Hascall VC, Erzurum SC, and Dweik RA. High levels of hyaluronan in idiopathic pulmonary arterial hypertension. *Am J Physiol Lung Cell Mol Physiol* 295: L789–L799, 2008.
2. Bauernfeind FG, Horvath G, Stutz A, Alnemri ES, MacDonald K, Speert D, Fernandes-Alnemri T, Wu J, Monks BG, Fitzgerald KA, Hornung V, and Latz E. Cutting edge: NF-kappaB activating pattern recognition and cytokine receptors license NLRP3 inflammasome activation by regulating NLRP3 expression. *J Immunol* 183: 787–791, 2009.
3. Bowler RP, Arcaroli J, Abraham E, Patel M, Chang LY, and Crapo JD. Evidence for extracellular superoxide dismutase as a mediator of hemorrhage-induced lung injury. *Am J Physiol Lung Cell Mol Physiol* 284: L680–L687, 2003.
4. Burke DL, Frid MG, Kunrath CL, Karoor V, Anwar A, Wagner BD, Strassheim D, and Stenmark KR. Sustained hypoxia promotes the development of a pulmonary artery-specific chronic inflammatory microenvironment. *Am J Physiol Lung Cell Mol Physiol* 297: L238–L250, 2009.
5. Chang LY and Crapo JD. Inhibition of airway inflammation and hyperreactivity by an antioxidant mimetic. *Free Radic Biol Med* 33: 379–386, 2002.
6. Chu Y, Iida S, Lund DD, Weiss RM, DiBona GF, Watanabe Y, Faraci FM, and Heistad DD. Gene transfer of extracellular superoxide dismutase reduces arterial pressure in spontaneously hypertensive rats: role of heparin-binding domain. *Circ Res* 92: 461–468, 2003.
7. Day BJ and Crapo JD. A metalloporphyrin superoxide dismutase mimetic protects against paraquat-induced lung injury *in vivo. Toxicol Appl Pharmacol* 140: 94–100, 1996.
8. Demarco VG, Whaley-Connell AT, Sowers JR, Habibi J, and Dellsperger KC. Contribution of oxidative stress to pulmonary arterial hypertension. *World J Cardiol* 2: 316–324, 2010.
9. Elmedal B, de Dam MY, Mulvany MJ, and Simonsen U. The superoxide dismutase mimetic, tempol, blunts right ventricular hypertrophy in chronic hypoxic rats. *Br J Pharmacol* 141: 105–113, 2004.
10. Franchi L, Eigenbrod T, Muñoz-Planillo R, and Nuñez G. The inflammasome: a caspase-1-activation platform that regulates immune responses and disease pathogenesis. *Nat Immunol* 10: 241–247, 2009.
11. Fujita H, Fujishima H, Chida S, Takahashi K, Qi Z, Kanetsuna Y, Breyer MD, Harris RC, Yamada Y, and Takahashi T. Reduction of renal superoxide dismutase in progressive diabetic nephropathy. *J Am Soc Nephrol* 20: 1303–1313, 2009.
12. Fukai T and Ushio-Fukai M. Superoxide Dismutases: Role in Redox Signaling, Vascular Function, and Diseases. *Antioxid Redox Signal* 7631: 1–76, 2011.
13. Gao F, Koenitzer JR, Tobolewski JM, Jiang D, Liang J, Noble PW, and Oury TD. Extracellular Superoxide Dismutase Inhibits Inflammation by Preventing Oxidative Fragmentation of Hyaluronan*. *J Biol Chem* 283: 6058–6066, 2008.
14. Giordano FJ. Review series oxygen, oxidative stress, hypoxia, and heart failure. *J Clin Invest* 115: 500–508, 2005.
15. Gongora MC, Lob HE, Landmesser U, Guzik TJ, Martin WD, Ozumi K, Wall SM, Wilson DS, Murthy N, Gravanis M, Fukai T, and Harrison DG. Loss of extracellular superoxide dismutase leads to acute lung damage in the presence of ambient air: a potential mechanism underlying adult respiratory distress syndrome. *Am J Pathol* 173: 915–926, 2008.
16. Hartney T, Birari R, Venkataraman S, Villegas L, Martinez M, Black SM, Stenmark KR, and Nozik-Grayck E. Xanthine

oxidase-derived ROS upregulate Egr-1 via ERK1/2 in PA smooth muscle cells; model to test impact of extracellular ROS in chronic hypoxia. *PloS one* 6: e27531-e27531, 2011.
17. Hassoun PM. Deciphering the "matrix" in pulmonary vascular remodelling. *Eur Respir J* 25: 778–779, 2005.
18. Hassoun PM, Mouthon L, Barbera JA, Eddahibi S, Flores SC, Grimminger F, Jones PL, Maitland ML, Michelakis ED, Morrell NW, Newman JH, Rabinovitch M, Schermuly R, Stenmark KR, Voelkel NF, Yuan JX, and Humbert M. Inflammation, growth factors, and pulmonary vascular remodeling, *J Am Coll Cardiol* 54: S10–S19, 2009.
19. Hoshino T, Okamoto M, Sakazaki Y, Kato S, Young HA, and Aizawa H. Role of proinflammatory cytokines IL-18 and IL-1beta in bleomycin-induced lung injury in humans and mice. *Am J Respir Cell Mol Biol* 41: 661–670, 2009.
20. Hynes RO. The extracellular matrix: not just pretty fibrils. *Science (New York N.Y.)* 326: 1216–1219, 2009.
21. Jankov RP, Kantores C, Pan J, and Belik J. Contribution of xanthine oxidase-derived superoxide to chronic hypoxic pulmonary hypertension in neonatal rats. *Am J Physiol Lung Cell Mol Physiol* 294: L233–L245, 2008.
22. Jiang D, Liang J, and Noble PW. Hyaluronan as an immune regulator in human diseases. *Physiol Rev* 91: 221–264, 2011.
23. Jiang D, Liang J, and Noble PW. Regulation of non-infectious lung injury, inflammation, and repair by the extracellular matrix glycosaminoglycan hyaluronan. *Anat Rec* 293: 982–985, 2010.
24. Kamezaki F, Tasaki H, Yamashita K, Tsutsui M, Koide S, Nakata S, Tanimoto A, Okazaki M, Sasaguri Y, Adachi T, and Otsuji Y. Gene transfer of extracellular superoxide dismutase ameliorates pulmonary hypertension in rats. *Am J Respir Crit Care Med* 177: 219–226, 2008.
25. Kim J, Shao Y, Kim SY, Kim S, Song HK, Jeon JH, Suh HW, Chung JW, and Yoon SR. Hypoxia-induced IL-18 Increases Hypoxia-inducible Factor-1a Expression through a Rac1-dependent NF-kB Pathway. *Mol Biol Cell* 19: 433–444, 2008.
26. Kinnula VL and Crapo JD. Superoxide dismutases in the lung and human lung diseases. *Am J Respir Crit Care Med* 167: 1600–1619, 2003.
27. Kliment CR and Oury TD. Oxidative stress, extracellular matrix targets, and idiopathic pulmonary fibrosis. *Free Radic Biol Med* 49: 707–717, 2010.
28. Kliment CR, Tobolewski JM, Manni ML, Tan RJ, Enghid J, and Oury TD. Extracellular superoxide dismutase protects against matrix degradation of heparan sulfate in the lung. *Antioxid Redox Signal* 10: 261–268, 2008.
29. Kvietys PR and Granger DN. Role of reactive oxygen and nitrogen species in the vascular responses to inflammation. *Free Radic Biol Med* 52: 556–592, 2012.
30. Lennon FE and Singleton PA. Role of hyaluronan and hyaluronan-binding proteins in lung pathobiology. *Am J Physiolo Lung Cell Mol Physiol* 301: L137–L147, 2011.
31. Martinon F. Activation mechanisms signaling by ROS drives inflammasome activation. *Immunology* 40: 616–619, 2010.
32. Nozik-Grayck E, Suliman HB, Majka S, Albietz J, Van Rheen Z, Roush K, and Stenmark KR. Lung EC-SOD overexpression attenuates hypoxic induction of Egr-1 and chronic hypoxic pulmonary vascular remodeling. *Am J Physiol Lung Cell Mol Physiol* 295: L422–L430, 2008.
33. Ogura Y, Sutterwala FS, and Flavell RA. The inflammasome: first line of the immune response to cell stress. *Cell* 126: 659–662, 2006.
34. Oury TD, Thakker K, Menache M, Chang LY, Crapo JD, and Day BJ. Attenuation of bleomycin-induced pulmonary fibrosis by a catalytic antioxidant metalloporphyrin. *Am J Respir Cell Mol Biol* 25: 164–169, 2001.
35. Papakonstantinou E, Kouri FM, Karakiulakis G, Klagas I, and Eickelberg O. Increased hyaluronic acid content in idiopathic pulmonary arterial hypertension. *Eur Respir J* 32: 1504–1512, 2008.
36. Patel M and Day BJ. Metalloporphyrin class of therapeutic catalytic antioxidants. *Trends Pharmacol Sci* 20: 359–364, 1999.
37. Rabinovitch M. Pathobiology of pulmonary hypertension. Extracellular matrix. *Clin Chest Med* 22: 433–449, viii, 2001.
38. Rashid M, Fahim M, and Kotwani A. Efficacy of tadalafil in chronic hypobaric hypoxia-induced pulmonary hypertension: possible mechanisms. *Fundam Clin Pharmacol,* 2012. [Epub ahead of print]; DOI: 10.1111/j.1472-8206.2011.01013.x.
39. Rashid M, Kotwani A, and Fahim M. Long-acting phosphodiesterase 5 inhibitor, tadalafil, and superoxide dismutase mimetic, tempol, protect against acute hypoxia-induced pulmonary hypertension in rats. *Hum Exp Toxicol* 31: 626–636, 2011.
40. Rees MD, Kennett EC, Whitelock JM, and Davies MJ. Oxidative damage to extracellular matrix and its role in human pathologies. *Free Radic Biol Med* 44: 1973–2001, 2008.
41. Soon E, Holmes AM, Treacy CM, Doughty NJ, Southgate L, Machado RD, Trembath RC, Jennings S, Barker L, Nicklin P, Walker C, Budd DC, Pepke-Zaba J, and Morrell NW. Elevated levels of inflammatory cytokines predict survival in idiopathic and familial pulmonary arterial hypertension. *Circulation* 122: 920–927, 2010.
42. Spasojević I, Chen Y, Noel TJ, Fan P, Zhang L, Rebouças JS, St Clair DK, and Batinić-Haberle I. Pharmacokinetics of the potent redox-modulating manganese porphyrin, MnTE-2-PyP(5+), in plasma and major organs of B6C3F1 mice. *Free Radi Biol Med* 45: 943–949, 2008.
43. Spasojević I, Chen Y, Noel TJ, Yu Y, Cole MP, Zhang L, Zhao Y, St Clair DK, and Batinic-Haberle I. Mn porphyrin-based superoxide dismutase (SOD) mimic, MnIIITE-2-PyP5+, targets mouse heart mitochondria. *Free Radic Biol Med* 42: 1193–1200, 2007.
44. Sugamura K and Keaney JF, Jr. Reactive oxygen species in cardiovascular disease. *Free Radic Biol Med* 51: 978–992, 2011.
45. Tschopp J and Schroder K. NLRP3 inflammasome activation: the convergence of multiple signalling pathways on ROS production? *Nat Rev Immunol* 10: 210–215, 2010.
46. Vergadi E, Chang MS, Lee C, Liang OD, Liu X, Fernandez-Gonzalez A, Mitsialis SA, and Kourembanas S. Early macrophage recruitment and alternative activation are critical for the later development of hypoxia-induced pulmonary hypertension. *Circulation* 123: 1986–1995, 2011.
47. Xu D, Guo H, Xu X, Lu Z, Fassett J, Hu X, Xu Y, Tang Q, Hu D, Somani A, Geurts A, Ostertag E, Bache RJ, Weir EK, and Chen Y. Exacerbated pulmonary arterial hypertension and right ventricular hypertrophy in animals with loss of function of extracellular superoxide dismutase. *Hypertension* 58: 303–309, 2011.
48. Yamasaki K, Muto J, Taylor KR, Cogen AL, Audish D, Bertin J, Grant EP, Coyle AJ, Misaghi A, Hoffman HM, and Gallo RL. NLRP3/cryopyrin is necessary for interleukin-1beta (IL-1beta) release in response to hyaluronan, an endogenous trigger of inflammation in response to injury. *J Biol Chem* 284: 12762–12771, 2009.
49. Yao H, Arunachalam G, Hwang J-W, Chung S, Sundar IK, Kinnula VL, Crapo JD, and Rahman I. Extracellular super-

oxide dismutase protects against pulmonary emphysema by attenuating oxidative fragmentation of ECM. *Proc Natl Acad Sci U S A* 107: 15571–15576, 2010.
50. Zelko IN and Folz RJ. Extracellular superoxide dismutase attenuates release of pulmonary hyaluronan from the extracellular matrix following bleomycin exposure. *FEBS Lett* 58: 1–6, 2010.

Address correspondence to:
Dr. Eva Nozik-Grayck
Department of Pediatrics
University of Colorado
Anschutz Medical Campus
12700 E. 19th Ave., B131
Aurora, CO 80045

E-mail: eva.grayck@ucdenver.edu

Date of first submission to ARS Central, July 9, 2012; date of final revised submission, November 26, 2012; date of acceptance, December 16, 2012.

Abbreviations Used

α-SMA = alpha smooth muscle actin
CHPH = chronic hypoxic pulmonary hypertension
ECM = extracellular matrix
EC-SOD = extracellular superoxide dismutase
HA = hyaluronan
Has1 = hyaluronan synthase
HPRT = hypoxanthine phosphoribosyltransferase 1
Hyal = hyaluronidase
IL-1β = interleukin 1-beta
MnTE-2-PyP = Mn(III)tetrakis(N-ethylpyridinium-2-yl) porphyrin
NALP3 = NACHT, LRR and PYD domain-containing protein 3
PAH = pulmonary arterial hypertension
PASMC = pulmonary artery smooth muscle cells
PBS = phosphate-buffered saline
PH = pulmonary hypertension
ROS = reactive oxygen species
RV = right ventricle
RVSP = right ventricular systolic pressure
SOD = superoxide dismutase